

## Absence of modulation of the expressed calcium channel $\alpha 1G$ subunit by $\alpha 2\delta$ subunits

L. Lacinová, N. Klugbauer and F. Hofmann

*Institut für Pharmakologie und Toxikologie der Technischen Universität München,  
Biedersteiner Straße 29, 80802 München, Germany*

(Received 10 December 1998; accepted after revision 15 January 1999)

1. The modulatory action of the  $\alpha 2\delta$  subunit on various high-voltage-activated calcium channels has been demonstrated previously. However, very little is known about auxiliary subunit modulation of low-voltage-activated (LVA) calcium channels. We have examined the modulation of the  $\alpha 1G$  subunit corresponding to the neuronal T-type calcium channel by the ubiquitously expressed  $\alpha 2\delta$ -1 and brain-specific  $\alpha 2\delta$ -3 subunits.
2. The  $\alpha 1G$  subunit was expressed alone or in combination with either the  $\alpha 2\delta$ -1 or  $\alpha 2\delta$ -3 subunit in human embryonic kidney (HEK 293) cells and whole-cell barium currents were measured. The current density–voltage relationships for peak and sustained current, kinetics of current activation and inactivation, voltage dependence of current inactivation and time course of the recovery from inactivation were analysed for each type of expressed channel. No significant difference was found for any of the examined parameters.
3. These results suggest that the LVA  $\alpha 1G$  channel is not regulated by known auxiliary  $\alpha 2\delta$  subunits.

Voltage-gated calcium channels have been purified and cloned from various tissues such as skeletal muscle, heart and brain. To date seven genes encoding  $\alpha 1$  subunits of the high-voltage-activated (HVA) and two genes of the low-voltage-activated (LVA) calcium channels have been identified (reviewed by Hofmann *et al.* 1994; Strom *et al.* 1998; Perez-Reyes *et al.* 1998; Cribbs *et al.* 1998). HVA calcium channels form hetero-oligomeric complexes consisting of various combinations of an  $\alpha 1$  protein with auxiliary  $\beta$ ,  $\alpha 2\delta$  and  $\gamma$  subunits. Modulation of HVA  $\alpha 1$  expression and biophysical parameters related to channel gating by diverse regulatory subunits have been studied extensively (reviewed by Walker & De Waard, 1998). Whether the LVA calcium channels have the same subunit composition as the HVA channels remains unclear.

LVA T-type calcium channels (neuronal  $\alpha 1G$  and cardiac  $\alpha 1H$ ) have only recently been cloned (Perez-Reyes *et al.* 1998; Cribbs *et al.* 1998; Klugbauer *et al.* 1998) and therefore analysis of regulation by auxiliary subunits was restricted previously to the manipulation of subunit expression in native cell lines. Lambert *et al.* (1997) and Leuranguer *et al.* (1998) employed antisense depletion of  $\beta$  subunits in nodus ganglion neurons or in the mammalian neuronal NG108-15 cell line, respectively, and showed that the  $\beta$  subunits had no effect on the T-type calcium channel. Wyatt *et al.* (1998) overexpressed  $\alpha 2\delta$  and neuronal  $\beta 2a$  subunits in

undifferentiated NG108-15 cells and reported the modulation of activation and inactivation of LVA calcium channels by the  $\alpha 2\delta$ , but not by the neuronal  $\beta 2a$ , subunit.

Functional coexpression of the  $\alpha 2\delta$  subunit with various combinations of  $\alpha 1$  and  $\beta$  subunits has been reported to result in an increase in the current amplitude, an acceleration of current activation, a shift of the current–voltage ( $I$ – $V$ ) curve in a hyperpolarizing direction and an acceleration of the time course of current inactivation of HVA calcium channels (Singer *et al.* 1991; De Waard & Campbell, 1995; Gurnett *et al.* 1996; Bangalore *et al.* 1996; Felix *et al.* 1997; Qin *et al.* 1998; Shirokov *et al.* 1998). All authors cited analysed the modulation of HVA channels by the only previously known  $\alpha 2\delta$  subunit,  $\alpha 2\delta$ -1. In addition to the  $\alpha 2\delta$ -1 subunit, two new subunits,  $\alpha 2\delta$ -2 and  $\alpha 2\delta$ -3, have been identified with 55 and 30% homology to  $\alpha 2\delta$ -1, respectively, and the neuronal  $\alpha 2\delta$ -3 subunit has been shown to modulate both  $\alpha 1C$  and  $\alpha 1E$  subunits (Klugbauer *et al.* 1999).

In this study we took advantage of cloned  $\alpha 1G$ , encoding a neuronal T-type calcium channel, and two  $\alpha 2\delta$  subunits: the ubiquitously expressed  $\alpha 2\delta$ -1 and neuronal  $\alpha 2\delta$ -3 subunits (Klugbauer *et al.* 1998, 1999). Upon functional expression in the human embryonic kidney (HEK 293) cell line, we show that the neuronal T-type calcium channel is not modulated by auxiliary  $\alpha 2\delta$  subunits.

## METHODS

### Cloning of calcium channel subunits

The mouse  $\alpha 1G$  calcium channel subunit was identified by a PCR-based approach with primers derived from the genomic sequence C54D2.5 of the nematode *Caenorhabditis elegans*, which encodes a putative calcium channel. This PCR product was used to screen a mouse brain cDNA library, which led to the identification of a full-length cDNA (Klugbauer *et al.* 1998). The GenBank accession number for mouse  $\alpha 1G$  is AJ012569.

The novel  $\alpha 2\delta$ -3 subunit was identified by an EST (expressed sequence tag) database search. An EST was found with the accession number AA190607, which had similarities with the  $\alpha 2\delta$  subunit of a calcium channel (Klugbauer *et al.* 1999). A PCR was performed to obtain a probe for screening a mouse brain cDNA library. The GenBank accession number for  $\alpha 2\delta$ -3 is AJ010949.

In each case the library clones were sequenced on both strands.

### Transfection of HEK 293 cells

The full-length cDNAs of all subunits, i.e.  $\alpha 1C$  (Biel *et al.* 1990),  $\alpha 1G$ ,  $\alpha 2\delta$ -1 (Mikami *et al.* 1989) and  $\alpha 2\delta$ -3 were cloned into the pcDNA 3 vector (Invitrogen). HEK 293 cells were transfected by lipofection with LipofectAMINE (Gibco BRL, Life Technologies) with the  $\alpha 1G$  subunit alone or with the  $\alpha 1G$  subunit together with one of the  $\alpha 2\delta$  subunits ( $\alpha 2\delta$ -1 or  $\alpha 2\delta$ -3). When two subunits were coexpressed, the DNA mass ratio was 1:1. Expression of  $\alpha 2\delta$  subunits was tested by parallel coexpression with the  $\alpha 1C$  channel using the same expression procedure and DNA concentration. For more details see Schuster *et al.* (1996).

### Electrophysiological recordings

Ionic currents from transfected cells were recorded using the whole-cell configuration of the patch clamp method. Barium was used as the charge carrier. The extracellular solution contained (mM): *N*-methyl-D-glucamine, 125; BaCl<sub>2</sub>, 20; CsCl, 5; MgCl<sub>2</sub>, 1; Hepes, 10; and glucose, 5; pH 7.4 (HCl). The intracellular solution contained (mM): CsCl, 60; CaCl<sub>2</sub>, 1; EGTA, 11; MgCl<sub>2</sub>, 1; K<sub>2</sub>ATP, 5; Hepes, 10; and aspartic acid, 50; pH 7.4 (CsOH). Currents were recorded using an EPC-9 patch clamp amplifier and corresponding Pulse software from HEKA Electronics (Lambrecht, Germany).

Patch pipettes were pulled from borosilicate glass. The pipette input resistance was typically between 1.8 and 2.2 M $\Omega$ . The capacity of individual cells ranged between 20 and 90 pF and series resistance ( $R_s$ ) ranged between 3.0 and 5.0 M $\Omega$ . Capacity transients were compensated using the built-in procedure of the HEKA system.

The holding potential ( $V_h$ ) in all experiments was  $-100$  mV. The  $I$ - $V$  relationship was measured by stepping to voltages between  $-80$  and  $+60$  mV for 40 ms at 0.2 Hz. Tail currents were analysed during 20 ms repolarizations to voltages between  $-90$  and  $-40$  mV following 5 ms depolarizations to  $-10$  mV at 0.2 Hz. Steady-state inactivation was measured by a series of 5 s prepulses to voltages between  $-120$  and  $-10$  mV, followed by a 10 ms return to  $V_h$  and a 40 ms test pulse to  $-10$  mV at 0.1 Hz. To analyse recovery from inactivation, the following pulse sequence was applied at 0.05 Hz: 40 ms test pulse to  $-10$  mV, 5 ms return to  $V_h$ , 5 s long inactivating pulse to 0 mV, return to  $V_h$  with variable length (recovery period), second test pulse identical to the first one. The recovery period ranged from 5 to 5120 ms.

For the fitting of time courses of activation, inactivation and deactivation measured traces were not leak subtracted. Similarly, all traces shown except for  $\alpha 1C$ -derived currents in Fig. 1B are raw records. The amplitude of the holding current at  $-100$  mV was typically less than 100 pA. For construction of the  $I$ - $V$  relationships shown in Figs 1A and 2A and C, leak current was subtracted using the  $P/4$  procedure.

Curve fittings were carried out using the Origin 5.0 software package (Microcal Inc., Northampton, MA, USA). The significance of observed differences was evaluated by Student's unpaired  $t$  test. A probability of 5% or less was considered to be significant. All experimental values are given as means  $\pm$  s.e.m.

## RESULTS

### Effect of $\alpha 2\delta$ -3 coexpression on voltage-dependent activation of the $\alpha 1C$ calcium channel

As a control for the expression procedure, the experiments with the  $\alpha 1C$  calcium channel were performed in parallel (see also Klugbauer *et al.* 1999). From the results shown in

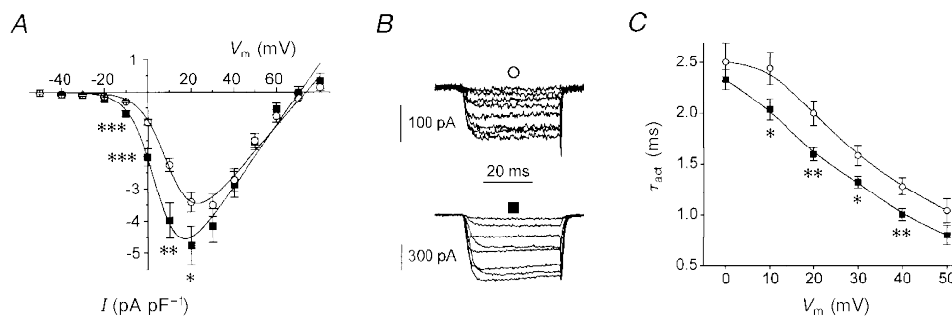


**Figure 1.** Effect of the  $\alpha 2\delta$ -3 subunit on the voltage dependence of  $\alpha 1C$  channel activation

A, mean current density–voltage ( $I$ - $V$ ) relationships for 14 cells transfected with the  $\alpha 1C$  subunit only (○) and 14 cells cotransfected with  $\alpha 1C$  and  $\alpha 2\delta$ -3 subunits (■). The continuous lines are fits of mean data to the modified Boltzmann equation (Table 1). \*  $P < 0.05$ , \*\*  $P < 0.01$ , \*\*\*  $P < 0.001$ , vs.  $\alpha 1C$  subunit only, Student's unpaired  $t$  test. B, examples of current records activated by voltage steps from the holding potential to voltages between  $-20$  and  $+50$  mV. ○,  $\alpha 1C$  channel, cell capacity 41 pF; ■,  $\alpha 1C + \alpha 2\delta$ -3 channel, cell capacity 79 pF. C,  $\tau_{act}$  represents the time constant of a monoexponential fit to the ascending part of the inward current activated by voltage steps to the indicated membrane potentials ( $V_m$ ). ○,  $\alpha 1C$  channel ( $n = 14$  cells); ■,  $\alpha 1C + \alpha 2\delta$ -3 channel ( $n = 14$  cells). \*  $P < 0.05$ , \*\*  $P < 0.01$ , vs.  $\alpha 1C$  subunit only, Student's unpaired  $t$  test.

**Table 1.** Effect of coexpression of  $\alpha 2\delta$ -1 and  $\alpha 2\delta$ -3 subunits on parameters of the current density–voltage relationship of the  $\alpha 1G$  channel

	<i>n</i>	$V_{rev}$ (mV)	$V_{0.5}$ (mV)	<i>k</i> (mV)
$\alpha 1C$	14	$73.6 \pm 1.7$	$10.6 \pm 1.3$	$6.2 \pm 0.9$
$\alpha 1C + \alpha 2\delta$ -3	14	$70.7 \pm 1.8$	$4.9 \pm 1.3^{**}$	$5.9 \pm 1.0$
$\alpha 1G$	9	$54.2 \pm 1.5$	$-28.4 \pm 0.6$	$4.0 \pm 0.6$
$\alpha 1G + \alpha 2\delta$ -1	10	$52.3 \pm 1.1$	$-28.1 \pm 0.5$	$4.4 \pm 0.4$
$\alpha 1G + \alpha 2\delta$ -3	11	$51.1 \pm 1.2$	$-29.8 \pm 0.5$	$4.1 \pm 0.5$

Peak *I*–*V* relationships shown in Figs 1*A* and 2*A* were fitted to a modified Boltzmann equation:  $I = G_{max}(V - V_{rev}) / (1 + \exp(-(V - V_{0.5})/k))$ , where  $G_{max}$  is maximum conductance,  $V_{rev}$  is the reversal potential,  $V_{0.5}$  is the potential of half-maximal current activation and *k* is the slope factor. *n*, number of experiments (cells). **\*\***  $P < 0.01$  vs.  $\alpha 1C$  subunit only, Student's unpaired *t* test.

Fig. 1 and Table 1 it can be seen that coexpression of the  $\alpha 2\delta$ -3 subunit together with  $\alpha 1C$  was sufficient to shift significantly the voltage dependence of barium current ( $I_{Ba}$ ) activation towards more negative membrane potentials (Fig. 1*A*) and to accelerate significantly the time course of current activation (Fig. 1*C*). Tail currents measured for  $\alpha 1C$  or  $\alpha 1C + \alpha 2\delta$ -3 channels were too fast to be evaluated accurately and therefore were not compared.

**Effect of  $\alpha 2\delta$ -1 or  $\alpha 2\delta$ -3 coexpression on biophysical parameters of *I*–*V* relationships of the  $\alpha 1G$  calcium channel**

When expressed in HEK 293 cells, the  $\alpha 1G$  subunit generated inward  $I_{Ba}$  which activated at about  $-40$  mV and reached a maximal peak amplitude at  $-10$  mV (Fig. 2*Aa*). Individual current traces exhibited fast and strongly voltage-dependent inactivation which resulted in the crossing of

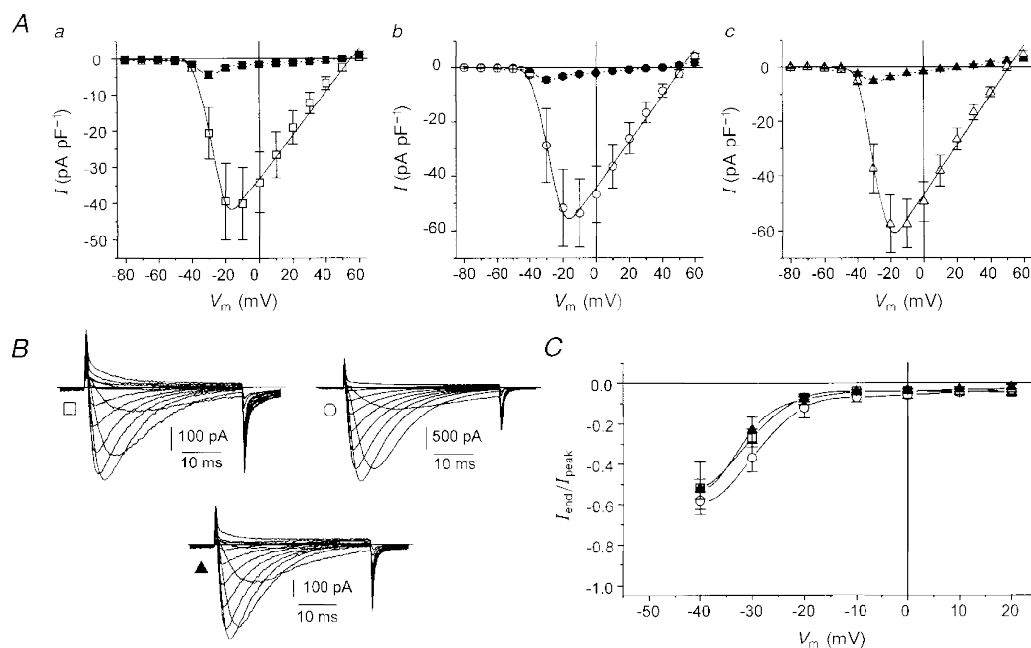


**Figure 2.** Voltage dependence of current activation

*A*, mean *I*–*V* relationships for 9 cells transfected with the  $\alpha 1G$  subunit only ( $\square$ ,  $\blacksquare$ ; *a*); 10 cells cotransfected with  $\alpha 1G$  and  $\alpha 2\delta$ -1 subunits ( $\circ$ ,  $\bullet$ ; *b*); and 11 cells cotransfected with  $\alpha 1G$  and  $\alpha 2\delta$ -3 subunits ( $\triangle$ ,  $\blacktriangle$ ; *c*). Open symbols represent peak current amplitude, filled symbols represent sustained current amplitude measured at 39 ms. Continuous lines connecting open symbols are fits of mean data to the modified Boltzmann equation (Table 1). *B*, examples of current records activated by steps to voltages between  $-50$  and  $+60$  mV.  $\square$ ,  $\alpha 1G$  channel, cell capacity 25 pF;  $\circ$ ,  $\alpha 1G + \alpha 2\delta$ -1 channel, cell capacity 58 pF;  $\blacktriangle$ ,  $\alpha 1G + \alpha 2\delta$ -3 channel, cell capacity 22 pF. *C*, *I*–*V* relationships for sustained current measured as described in *A*. Current amplitudes at 39 ms ( $I_{end}$ ) were first normalized to the peak current amplitude ( $I_{peak}$ ) of each trace and then averaged. Symbols as in *B*.

successive current traces (Fig. 2B) and in a very small amplitude of current sustained after 39 ms of depolarization. As a result of the rapid increase in the speed of voltage-dependent inactivation during the first two suprathreshold depolarizations, the sustained current reached a maximal amplitude at  $-30$  mV, i.e. 20 mV earlier than the peak current (Fig. 2Aa). These features are considered to be a signature pattern for the LVA T-type calcium channel and confirm that the subunit encodes a member of the neuronal LVA channel family. Upon coexpression of the  $\alpha 2\delta$ -1 or  $\alpha 2\delta$ -3 subunit, none of the above mentioned characteristics of expressed channels changed (Fig. 2Ab, Ac and B). The mean expressed current densities were  $-40.1 \pm 9.9$  pA pF $^{-1}$  for the  $\alpha 1G$  channel,  $-53.6 \pm 12.4$  pA pF $^{-1}$  for the  $\alpha 1G + \alpha 2\delta$ -1 channel and  $-57.6 \pm 10.4$  pA pF $^{-1}$  for the  $\alpha 1G + \alpha 2\delta$ -3 channel. These values are not significantly different. Parameters characterizing the voltage dependence of current activation, i.e. reversal potential ( $V_{rev}$ ), potential of half-maximal current activation ( $V_{0.5}$ ) and the slope factor  $k$  were not significantly affected by coexpression of either  $\alpha 2\delta$  subunit (Table 1). To facilitate comparison of the voltage

dependence of current maintained after 39 ms of depolarization, the amplitudes of maintained current were normalized to the peak amplitude of individual current traces.  $I$ - $V$  relationships for all channel types virtually overlapped (Fig. 2C).

The characteristics of  $I_{Ba}$  carried through channels formed from the  $\alpha 1G$  subunit alone or from  $\alpha 1G$  in combination with either of the  $\alpha 2\delta$  subunits were comparable to those reported by Perez-Reyes *et al.* (1998) upon expression of the  $\alpha 1G$  channel in *Xenopus* oocytes. The shift by +10 mV along the voltage axis is most probably caused by the higher concentration of charge carrier (20 vs. 10 mM Ba $^{2+}$ ) used in our experiments. The steeper slope of voltage dependence of current activation in our study may be due to a voltage drop on non-compensated  $R_s$ . This usually ranged between 2.5 and 10 mV (the highest value of  $R_s$  was 5 M $\Omega$  and the  $I_{Ba}$  amplitude typically ranged between 0.5 and 2 nA). However, because these values were unaltered upon coexpression of  $\alpha 2\delta$  subunits, the comparison of voltage-dependent parameters was not affected.

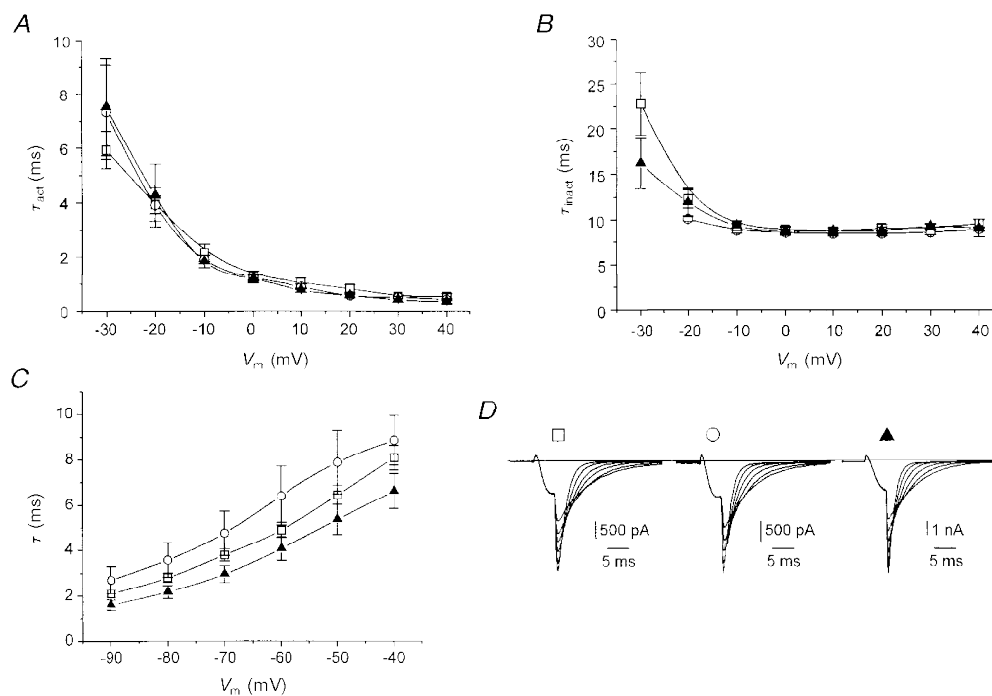


**Figure 3.** Time and voltage dependence of current activation, inactivation and deactivation

A,  $\tau_{act}$  represents the time constant of a monoexponential fit to the ascending part of the current activated by voltage steps to the indicated membrane potentials.  $\square$ ,  $\alpha 1G$  channel ( $n = 9$  cells);  $\circ$ ,  $\alpha 1G + \alpha 2\delta$ -1 channel ( $n = 10$  cells);  $\blacktriangle$ ,  $\alpha 1G + \alpha 2\delta$ -3 channel ( $n = 11$  cells). B,  $\tau_{inact}$  represents the time constant of a monoexponential fit to the descending part of the current activated by voltage steps to the indicated membrane potentials.  $\square$ ,  $\alpha 1G$  channel ( $n = 9$  cells);  $\circ$ ,  $\alpha 1G + \alpha 2\delta$ -1 channel ( $n = 10$  cells);  $\blacktriangle$ ,  $\alpha 1G + \alpha 2\delta$ -3 channel ( $n = 11$  cells). C, time constants of current decay evaluated by monoexponential fits of tail currents measured after repolarization to membrane voltages indicated.  $\square$ ,  $\alpha 1G$  channel ( $n = 7$  cells);  $\circ$ ,  $\alpha 1G + \alpha 2\delta$ -1 channel ( $n = 4$  cells);  $\blacktriangle$ ,  $\alpha 1G + \alpha 2\delta$ -3 channel ( $n = 8$  cells). D, examples of tail current records.  $\square$ ,  $\alpha 1G$  channel, cell capacity 33 pF;  $\circ$ ,  $\alpha 1G + \alpha 2\delta$ -1 channel, cell capacity 36 pF;  $\blacktriangle$ ,  $\alpha 1G + \alpha 2\delta$ -3 channel, cell capacity 37 pF.

### Effect of $\alpha 2\delta$ -1 or $\alpha 2\delta$ -3 coexpression on the time and voltage dependence of activation, inactivation and deactivation of the current through the $\alpha 1G$ calcium channel

To compare the time courses of current activation we fitted the current trace between the intercept with the zero current line and the small plateau around the current peak with a single exponential. The time constants for current activation ( $\tau_{act}$ ) decreased with increasing membrane potential over the entire tested interval of voltages (Fig. 3A). At each tested membrane potential, values of  $\tau_{act}$  were not significantly different between  $\alpha 1G$ ,  $\alpha 1G + \alpha 2\delta$ -1 and  $\alpha 1G + \alpha 2\delta$ -3 channels.

The time courses of current inactivation during the depolarizing step could be fitted with a single exponential. The time constants for current inactivation ( $\tau_{inact}$ ) decreased rapidly during the first two suprathreshold pulses and

afterwards remained constant (Fig. 3B). Similar to the activation time constants,  $\tau_{inact}$  was not significantly different between  $\alpha 1G$ ,  $\alpha 1G + \alpha 2\delta$ -1 and  $\alpha 1G + \alpha 2\delta$ -3 channels.

Another distinctive characteristic of T-type calcium channel gating is slow kinetics of deactivation, which can be measured as the time constant of tail current decay. We compared the time constants of tail current decay of  $\alpha 1G$ ,  $\alpha 1G + \alpha 2\delta$ -1 and  $\alpha 1G + \alpha 2\delta$ -3 channels at repolarizing potentials ranging from  $-90$  to  $-40$  mV (Fig. 3C and D). No significant difference amongst the three combinations was found.

### Effect of $\alpha 2\delta$ -1 or $\alpha 2\delta$ -3 coexpression on steady-state inactivation and recovery from inactivation of the current through the $\alpha 1G$ calcium channel

The dependence of channel availability on the resting membrane potential was tested using a 5 s conditioning

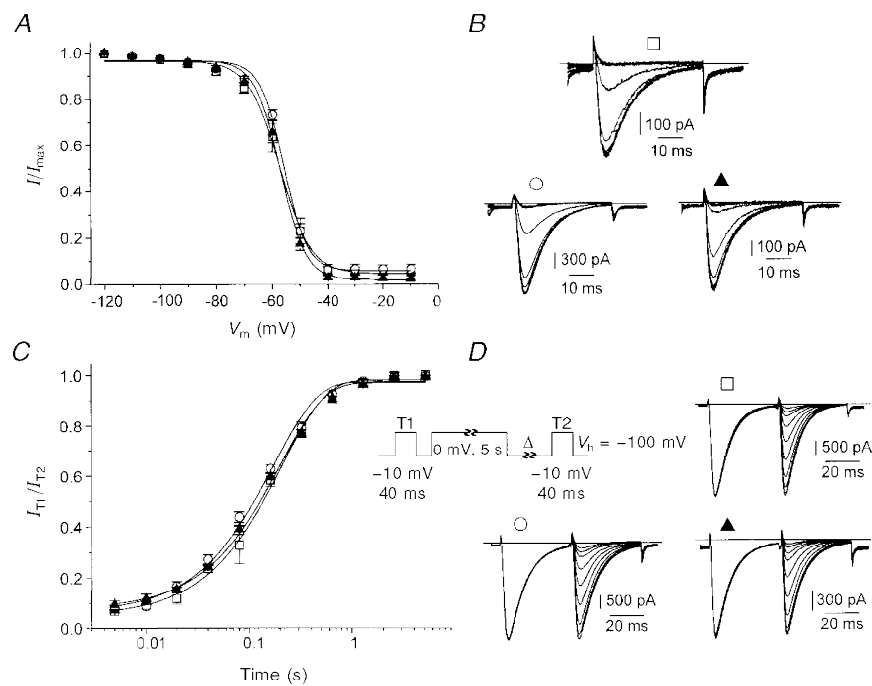


**Figure 4.** Voltage dependence of current availability and time course of recovery from voltage-dependent inactivation

A, steady-state inactivation curves for  $\alpha 1G$  ( $\square$ ,  $n = 8$  cells),  $\alpha 1G + \alpha 2\delta$ -1 ( $\circ$ ,  $n = 9$  cells) and  $\alpha 1G + \alpha 2\delta$ -3 ( $\blacktriangle$ ,  $n = 10$  cells) channels. Continuous lines represent the fits of experimental points to the Boltzmann equation. Resulting  $V_{0.5}$  (potential of half-maximal current inactivation) and  $k$  values were  $-57.3 \pm 0.6$  mV and  $5.6 \pm 0.5$  mV for the  $\alpha 1G$  channel,  $-55.9 \pm 0.6$  mV and  $4.2 \pm 0.4$  mV for the  $\alpha 1G + \alpha 2\delta$ -1 channel and  $-57.2 \pm 0.5$  mV and  $4.6 \pm 0.9$  mV for the  $\alpha 1G + \alpha 2\delta$ -3 channel. B, examples of currents measured during the steady-state inactivation protocol.  $\square$ ,  $\alpha 1G$  channel, cell capacity 25 pF;  $\circ$ ,  $\alpha 1G + \alpha 2\delta$ -1 channel, cell capacity 92 pF;  $\blacktriangle$ ,  $\alpha 1G + \alpha 2\delta$ -3 channel, cell capacity 22 pF. C, proportion of current available during the second test pulse T2 plotted against recovery time ( $\Delta$ ). The voltage protocol is shown in the inset;  $V_h$ , holding potential. Continuous lines represent monoexponential fits to the experimental points. Individual time constants of recovery were  $202 \pm 17$  ms for the  $\alpha 1G$  channel ( $\square$ ,  $n = 5$  cells),  $171 \pm 15$  ms for the  $\alpha 1G + \alpha 2\delta$ -1 channel ( $\circ$ ,  $n = 4$  cells) and  $206 \pm 18$  ms for the  $\alpha 1G + \alpha 2\delta$ -3 channel ( $\blacktriangle$ ,  $n = 7$  cells). D, examples of currents measured during both test pulses T1 and T2. The interval between the two test pulses was omitted.  $\square$ ,  $\alpha 1G$  channel, cell capacity 38 pF;  $\circ$ ,  $\alpha 1G + \alpha 2\delta$ -1 channel, cell capacity 37 pF;  $\blacktriangle$ ,  $\alpha 1G + \alpha 2\delta$ -3 channel, cell capacity 23 pF.



prepulse (Fig. 4A). Considering that the time constants of  $I_{Ba}$  inactivation were approximately 10 ms at most membrane potentials (Fig. 3B) we assumed that this length of prepulse would be sufficient to obtain steady-state inactivation. At each membrane potential the proportion of non-inactivated channels was virtually identical for all three channels and the  $V_{0.5}$  (potential of half-maximal inactivation) values calculated from fits to the Boltzmann equation were very similar. Nevertheless, close inspection of Fig. 4A revealed slight differences in the slopes of the steady-state inactivation curves. The slope values were significantly different between  $\alpha 1G$  and  $\alpha 1G + \alpha 2\delta-1$  channels ( $P < 0.05$ ). This deviation in slope values was the only significant difference found in all analyses performed. However, considering the sharp steepness of all three curves and the fact that the relative number of available channels do not differ at any prepulse voltage this difference has no functional implications for the channel gating.

The recovery from voltage-dependent inactivation of the  $\alpha 1G$  channel was monoexponential and was complete in less than 2 s (Fig. 4C). Coexpression of either  $\alpha 2\delta-1$  or  $\alpha 2\delta-3$  did not significantly affect the recovery time constant.

## DISCUSSION

This study was undertaken to investigate whether the neuronal  $\alpha 1G$  calcium channel is modulated by two different auxiliary  $\alpha 2\delta$  subunits. Our results show that the  $\alpha 1G$  channel is not regulated by either the  $\alpha 2\delta-1$  or  $\alpha 2\delta-3$  subunit.

Lack of modulation of  $\alpha 1G$  channels by auxiliary subunits would be an exception amongst the calcium channels. All HVA calcium channels identified so far, i.e.  $\alpha 1A$ ,  $\alpha 1B$ ,  $\alpha 1C$ ,  $\alpha 1D$  and  $\alpha 1S$  and the  $\alpha 1E$  channel (which has some properties similar to those of the LVA channel) have been shown to be modulated by auxiliary subunits (reviewed by Walker & De Waard, 1998). When the above mentioned  $\alpha 1$  subunits are expressed alone, either in *Xenopus* oocytes or in mammalian cell lines, their gating-related properties differ from the properties of their native analogues. The time dependence of channel inactivation is particularly slow for HVA  $\alpha 1$  channels when compared with that of their native counterparts. This deviation is relieved by coexpression of auxiliary subunits (for review see Walker & De Waard, 1998).

In contrast, the current conducted by expressed  $\alpha 1G$  subunits is very similar to that of neuronal T-type calcium channels (reviewed by Huguenard, 1996; Randall & Tsien, 1997; Lambert *et al.* 1997; Leuranguer *et al.* 1998; Wyatt *et al.* 1998). It is therefore possible that T-type calcium channels are not associated with regulatory subunits. Indeed, the amino acid sequence of the  $\alpha 1G$  subunit supports the notion that this channel is not modulated by  $\beta$  subunits (Perez-Reyes *et al.* 1998; Cribbs *et al.* 1998; Klugbauer *et al.* 1998) since the connector between the I and II repeats lacks the sequence identified as a binding site for the  $\beta$  subunit. This

suggestion is supported by the work of Lambert *et al.* (1997) and Leuranguer *et al.* (1998) who have shown that the neuronal T-type calcium channel is not affected by antisense depletion of known  $\beta$  subunits.

Regulation of the kinetics of channel activation and inactivation has been attributed to the transmembrane  $\delta$  segment of the  $\alpha 2\delta$  subunit (Felix *et al.* 1997). The corresponding interaction region on the  $\alpha 1$  subunit has not yet been identified and therefore no suggestions can be derived from the  $\alpha 1G$  sequence. Nevertheless, coexpression of the  $\alpha 2\delta-1$  subunit with the  $\alpha 1G$  subunit performed in this work did not alter any gating-related biophysical parameter of the  $\alpha 1G$  channel.

In addition to the first known  $\alpha 2\delta$  subunit,  $\alpha 2\delta-1$ , two new subunits,  $\alpha 2\delta-2$  and  $\alpha 2\delta-3$ , have been identified, which show 55 and 30% homology with  $\alpha 2\delta-1$ , respectively (Klugbauer *et al.* 1998). Because the  $\alpha 2\delta-3$  subunit is expressed specifically in brain, it was considered possible that it may have a specific function in the regulation of  $\alpha 1G$  and/or other neuronal calcium channels. The  $\alpha 2\delta-3$  subunit was shown to be partially specific to the neuronal  $\alpha 1E$  channel compared with the ubiquitously expressed  $\alpha 1C$  channel (Klugbauer *et al.* 1999). As we have shown here,  $\alpha 2\delta-3$  also failed to influence the  $\alpha 1G$  channel.

In contrast to our results, Wyatt *et al.* (1998) recently reported the effects of the  $\alpha 2\delta$  subunit on voltage-dependent activation and the sustained component of T-type calcium channels in the mammalian NG108-15 cell line. Even if the current measured by Wyatt *et al.* (1998) was predominantly a T-type calcium current, immunostaining of undifferentiated NG108-15 cells confirmed the presence of  $\alpha 1A$ ,  $\alpha 1B$ ,  $\alpha 1C$ ,  $\alpha 1D$  and  $\alpha 1E$  proteins. Staining for  $\alpha 1C$  was very weak with little membrane association (Wyatt *et al.* 1998). The  $\alpha 2\delta$  subunit is known to facilitate membrane trafficking of the  $\alpha 1C$  subunit (Shistik *et al.* 1995). It is therefore possible that the non-inactivated current component which Wyatt *et al.* (1998) observed upon coexpression of the  $\alpha 2\delta$  subunit during depolarizing pulses positive to  $-30$  mV reflects the upregulation of previously unmeasurable L-type calcium channels.

To summarize, the results of this study suggest that the expressed neuronal  $\alpha 1G$  channel is not regulated by  $\alpha 2\delta-1$  or  $\alpha 2\delta-3$  subunits. Together with the work of Lambert *et al.* (1997) and Leuranguer *et al.* (1998), we may conclude that the biophysical properties of neuronal T-type calcium channels are not regulated by presently known auxiliary subunits of the HVA channel. We cannot exclude the possibility that  $\alpha 2\delta$  subunits do associate with the  $\alpha 1G$  subunit without affecting current characteristics under control conditions, but that they may regulate its pharmacological properties. Also, the possibility of regulation of T-type calcium channels by a not yet identified class of subunits remains open.

- BANGALORE, R., MEHRKE, G., GINGRICH, K., HOFMANN, F. & KASS, R. S. (1996). Influence of L-type Ca channel  $\alpha_2/\delta$ -subunit on ionic and gating current in transiently transfected HEK 293 cells. *American Journal of Physiology* **270**, H1521–1528.
- BIEL, M., RUTH, P., BOSSE, E., HULLIN, R., STÜHMER, W., FLOCKERZI, V. & HOFMANN, F. (1990). Primary structure and functional expression of a high voltage activated calcium channel from rabbit lung. *FEBS Letters* **269**, 409–412.
- CRIBBS, L. L., LEE, J.-H., YANG, J., SATIN, J., ZHANG, Y., DAUD, A., BARCLAY, J., WILLIAMSON, M. P., FOX, M., REES, M. & PEREZ-REYES, E. (1998). Cloning and characterization of  $\alpha 1H$  from human heart, a member of the T-type  $Ca^{2+}$  channel gene family. *Circulation Research* **83**, 103–109.
- DE WAARD, M. & CAMPBELL, K. P. (1995). Subunit regulation of the neuronal  $\alpha_{1A}$   $Ca^{2+}$  channel expressed in *Xenopus* oocytes. *Journal of Physiology* **485**, 619–634.
- FELIX, R., GURNETT, C. A., DE WAARD, M. & CAMPBELL, K. P. (1997). Dissection of functional domains of the voltage-dependent  $Ca^{2+}$  channel  $\alpha_2\delta$  subunit. *Journal of Neuroscience* **17**, 6884–6891.
- GURNETT, C. A., DE WAARD, M. & CAMPBELL, K. P. (1996). Dual function of the voltage-dependent  $Ca^{2+}$   $\alpha_2\delta$  subunit in current stimulation and subunit interaction. *Neuron* **16**, 431–440.
- HOFMANN, F., BIEL, M. & FLOCKERZI, V. (1994). Molecular basis for  $Ca^{2+}$  channel diversity. *Annual Review of Neuroscience* **17**, 399–418.
- HUGUENARD, J. R. (1996). Low-threshold calcium currents in central nervous system neurons. *Annual Review of Physiology* **58**, 329–348.
- KLUGBAUER, N., LACINOVÁ, L. & HOFMANN, F. (1998). Identification of novel subunits of the voltage gated calcium channel family. *Naunyn-Schmiedeberg's Archives of Pharmacology* **358** (suppl. 1), R687.
- KLUGBAUER, N., LACINOVÁ, L., MARAIS, E., HOBOM, M. & HOFMANN, F. (1999). Molecular diversity of the calcium channel  $\alpha_2\delta$  subunit. *Journal of Neuroscience* **19**, 684–691.
- LAMBERT, R. C., MAULET, Y., MOUTON, J., BEATIE, R., VOLSEN, S., DE WAARD, M. & FELTZ, A. (1997). T-type  $Ca^{2+}$  current properties are not modified by  $Ca^{2+}$  channel  $\beta$  subunit depletion in nodus ganglion neurons. *Journal of Neuroscience* **17**, 6621–6628.
- LEURANGUER, V., BOURINET, E., LORY, P. & NARGEOT, J. (1998). Antisense depletion of  $\beta$ -subunits fails to affect T-type calcium channels properties in a neuroblastoma cell line. *Neuropharmacology* **37**, 701–708.
- MIKAMI, A., IMOTO, K., TANABE, T., NIIDOME, T., MORI, Y., TAKESHIMA, H., NARUMIYA, S. & NUMA, S. (1989). Primary structure and functional expression of the cardiac dihydropyridine-sensitive calcium channel. *Nature* **340**, 230–233.
- PEREZ-REYES, E., CRIBBS, L. L., DAUD, A., LACERDA, A. E., BARCLAY, J., WILLIAMSON, M. P., FOX, M., REES, M. & LEE, J.-H. (1998). Molecular characterization of a neuronal low-voltage-activated T-type calcium channel. *Nature* **391**, 896–899.
- QIN, N., OLCESE, R., STEFANI, E. & BIRNBAUMER, L. (1998). Modulation of human neuronal  $\alpha_{1E}$ -type calcium channel by  $\alpha_2\delta$ -subunit. *American Journal of Physiology* **274**, C1324–1331.
- RANDALL, A. D. & TSIEN, R. W. (1997). Contrasting biophysical and pharmacological properties of T-type and R-type calcium channels. *Neuropharmacology* **36**, 879–893.
- SCHUSTER, A., LACINOVÁ, L., KLUGBAUER, N., ITO, H., BIRNBAUMER, L. & HOFMANN, F. (1996). The IVS6 segment of the L-type calcium channel is critical for the action of dihydropyridines and phenylalkylamines. *EMBO Journal* **15**, 2365–2370.
- SHIROKOV, R., FERREIRA, G., YI, J. & RÍOS, E. (1998). Inactivation of gating currents of L-type calcium channels. Specific role of the  $\alpha_2\delta$  subunit. *Journal of General Physiology* **111**, 807–823.
- SHISTIK, E., IVANINA, T., PURI, T., HOSEY, M. & DASCAL, N. (1995).  $Ca^{2+}$  current enhancement by  $\alpha 2/\delta$  and  $\beta$  subunits in *Xenopus* oocytes: contribution of changes in channel gating and  $\alpha 1$  protein level. *Journal of Physiology* **489**, 55–62.
- SINGER, D., BIEL, M., LOTAN, I., FLOCKERZI, V., HOFMANN, F. & DASCAL, N. (1991). The roles of the subunits in the function of the calcium channel. *Science* **253**, 1553–1557.
- STROM, T. M., NYAKATURA, G., APFELSTEDT-SYLLA, E., HELLEBRAND, H., LORENZ, B., WEBER, B. H., WUTZ, K., GUTWILLINGER, N., RUTHER, K., DRESCHER, B., SAUER, C., ZRENNER, E., MEITINGER, T., ROSENTHAL, A. & MEINDL, A. (1998). An L-type calcium-channel gene mutated in incomplete X-linked congenital stationary night blindness. *Nature Genetics* **19**, 260–263.
- WALKER, D. & DE WAARD, M. (1998). Subunit interaction sites in voltage-dependent  $Ca^{2+}$  channels: role in channel function. *Trends in Neurosciences* **21**, 148–154.
- WYATT, C. N., PAGE, K. M., BERROW, N. S., BRICE, N. L. & DOLPHIN, A. C. (1998). The effect of overexpression of auxiliary  $Ca^{2+}$  channel subunits on native  $Ca^{2+}$  channel currents in undifferentiated mammalian NG108-15 cells. *Journal of Physiology* **510**, 347–360.

#### Acknowledgements

This work was supported by the Deutsche Forschungsgemeinschaft and Fond der Chemie.

#### Corresponding author

L. Lacinová: Institut für Pharmakologie und Toxikologie der Technischen Universität München, Biedersteiner Straße 29, 80802 München, Germany.

Email: lacinova@ipt.med.tu-muenchen.de

L. Lacinová was on leave from the Institute of Molecular Physiology and Genetics, Slovak Academy of Sciences, Vlarska 5, 833 04 Bratislava, Slovakia.